

**TECHNICAL TRANSACTIONS**  
ENVIRONMENTAL ENGINEERING**CZASOPISMO TECHNICZNE**  
ŚRODOWISKO

2-Ś/2015

ALEKSANDER URBAŃSKI\*, LESZEK OPYRCHAŁ\*\*

## ANALYSIS OF MECHANICAL EFFECTS OF LOW- AND HIGH-FREQUENCY TEMPERATURE CHANGES IN A MASSIVE CONCRETE DAM

### ANALIZA WPŁYWU WOLNO- I SZYBKOSMIENNYCH PÓŁ TEMPERATURY NA STAN MECHANICZNY MASYWNEJ ZAPORY BETONOWEJ

#### Abstract

The numerical simulation of time evolution of thermal and mechanical fields in a selected section of a massive concrete dam was undertaken by means of the Finite Element Method (FEM) using 3D modelling. Low- (i.e. with time period – year) and high frequency (i.e. with time period – day) cycles of environment temperature variation were considered. The results of the computation confirmed the hypothesis of the vulnerability of the structure to thermal influences and explained the mechanism of the structural defects observed.

*Keywords: thermo-mechanical effects, massive concrete dam, FEM*

#### Streszczenie

W pracy przedstawiono symulacje numeryczne dotyczące efektów termo-mechanicznych w masywnej zaporce betonowej. Zastosowano trójwymiarowe modelowanie metodą elementów skończonych niestacjonarnego w czasie pola temperatury i pól mechanicznych. Rozpatrzono zarówno wpływ zmian temperatury otoczenia w cyklu rocznym, jak i w cyklu dobowym. Wykazano, że mogą być one przyczyną zaobserwowanych uszkodzeń na powierzchniach betonu.

*Słowa kluczowe: efekty termo-mechaniczne, masywna zapora betonowa, MES*

**DOI: 10.4467/2353737XCT.15.235.4621**

\* Prof. DSc. PhD. Aleksander Urbański, Institute of Geotechnics, Faculty of Environmental Engineering, Cracow University of Technology.

\*\* DSc. PhD. Leszek Opyrchal, AGH University of Science and Technology, Faculty of Mining Surveying and Environmental Engineering, Department of Environmental Management and Protection.

## Symbols

$T$  – temperature [K]

$t$  – time [day]

## 1. Introduction

The dam is located in the southwest Poland. The reservoir area is 32 ha and water volume is 2 mln m<sup>3</sup>. The total length of the dam is 306.0 m. Its central part is split into 12 sections of buttress type concrete dam with variable height, ranging from 15.0 to 34.5 m in the middle.

In the year 1998 [3], i.e. after 34 years of exploitation, cracks and fissures in the buttress and transition zones of the highest sections of the dam (nr 6 and 7), as shown in Fig. 1, were noted during a technical inspection. In the year 2013 surface cracking of the concrete was also detected on the head surfaces of the buttress. An explanation for the observed phenomena has become vital for the safety assessment of the dam and design of the rehabilitation procedure. The crack pattern indicates that the possible reason for cracking is the influence of the thermal stress field.

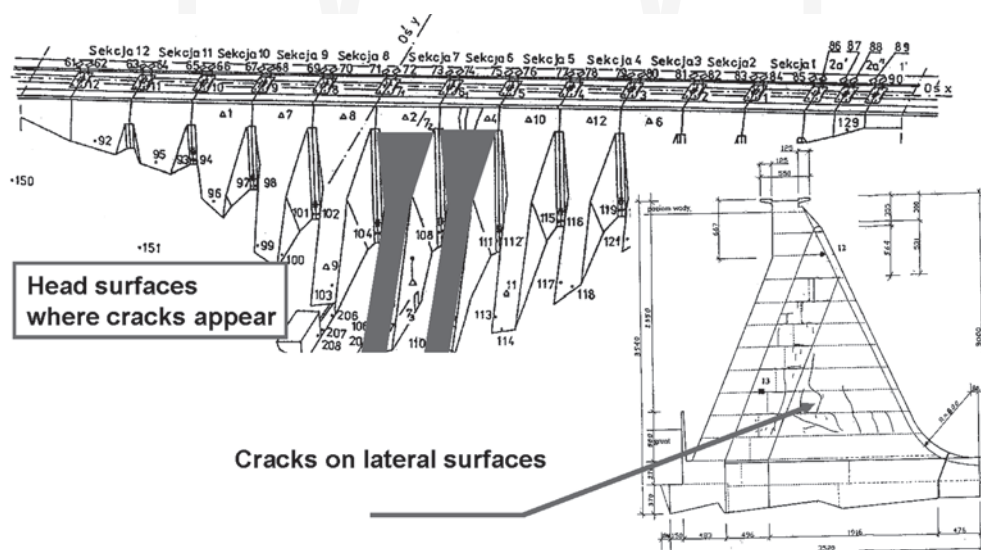


Fig. 1. a) View of the dam from the downstream site b) View of the right wall of the buttress of the 6-th section of the dam with cracks, after [3].

Typical cracks appearing on the head surface of the buttress are shown in Fig. 2.



Fig. 2. Crack on the head surface

## 2. Numerical modelling of the thermal process and its mechanical effects in a massive concrete structure

As an initial investigation of the observed cracks points to a thermal stress field as the most probable cause, numerical simulation of the time evolution of thermal and mechanical fields in the highest central section of the dam was undertaken using the Finite Element Method (FEM).

As a software tool, the Z\_SOIL.PC system was chosen [2, 4], because of its ability to take into account in a fully automated way the interaction between: temperature evaluated in a transient heat transfer problem, pore pressure field developed in filtration analysis with materially nonlinear and/or rheological static analysis of the concrete dam and its foundation.

Due to the generic tri-dimensionality of the dam section, a full 3D FEM simulation has been created. The strategy for the analysis was adopted as summarized below. Firstly, thermal analysis of yearly (low-frequency) environmental temperature variation was undertaken. Its results, i.e. temperature space and time distribution  $T(\mathbf{x}, t)$ , consist of an entry to the analysis of mechanical fields (displacements, strains and stresses). These analyses were run for a total period of 10 years, what is necessary to remove the effects of an improperly set thermal initial condition (as it is *a-priori* unknown). A time step of  $dt1 = 10$  days was assumed, thus only low-frequency (winter-summer) environmental temperature variation could be taken into account.

Secondly, the influence of a high-frequency, i.e. daily (night-day) cycle of environmental temperature variation and its mechanical effects were analysed separately, for the fragment of the structure close to the cracked head surface, for a period of 1 year with time stepping  $dt2 = 0.1$  day. Of course, this analysis takes into account (as initial and boundary conditions) the temperatures obtained in the first, low-frequency analysis.

For both cases an incremental mechanical analysis is run, taking into account the increments of the imposed thermally induced strains. Note that these strains, in general, do

not fulfil the Saint-Venant compatibility equations, and as so are the source of self-equilibrate stresses.

As numerical evaluation of all integrals over a finite element (for stiffness or force vector) requires values at integration (Gauss) points, temperature increments at these points are interpolated from values previously evaluated at the nodes of the FE mesh used in the heat problem. Notice that the FE meshes used in both thermal and mechanical analyses do not need to be identical; the same holds for time step implementation, see [2] for details.

In this way, using the described two-stage analysis it was possible to explain all the mechanisms of observed cracks in the structure. The analysis of high-frequency temperature changes for the full model of the section, which also requires much denser FE discretisation, is currently not feasible on standard PC computers, due to the numerical size of the job.

The mechanical material parameters of the concrete were assumed as follows, marked with (\*) basing on the measurements done on core samples (diameter 75 mm, length 150mm): Young's modulus:  $E = 21.2$  GPa (\*), Poisson's ratio:  $\nu = 0.19$  (\*), tensile strength:  $f_t = 3.000$  MPa (\*, Brazilian test), compressive strength  $f_c = 30.000$  MPa (\*), thermal dilatancy coefficient:  $\alpha = 1.13 \cdot 10^{-5}$  [1/K].

For the concrete elastic-perfectly plastic model due to Menetrey and Willam (MW) [1], with limit surface tri-elliptic in axiatoric and parabolic in deviatoric section, identified from uniaxial tensile ( $f_t$ ) and compressive strength ( $f_c$ ) was applied.

## 2.1. Thermal and mechanical analysis of yearly (low-frequency) environmental temperature variation

The first problem to be solved is to find the space distribution and time evolution of the temperature field  $T(\mathbf{x}, t)$  in the concrete dam section and its surroundings due to the annual cyclic variation of climatic conditions described by the Fourier equation (1):

$$(\lambda (T_i))_{,i} = c \dot{T} \quad (1)$$

where: heat conductivity  $\lambda = 155/259$  [kJ/(m · day · K)] for concrete/bedrock and heat capacity  $c = 2016 / 1800$  [kJ/(m<sup>3</sup> · K)], respectively, were assumed.

In the analysis, all 3 types of boundary conditions (BC) were used (Fig.3a):

1. Known temperature BC (1st kind),  $T(\mathbf{x}, t) = \bar{T}(h, t)$  at the dam upstream surface. Starting from the measured water temperature profiles as a function of the depth  $h$  in winter  $T_w(h)$  and in summer  $T_s(h)$ , assuming sinusoidal time variability in the temperature during the yearly cycle the relation is used, ( $t = 0$  set for 1st of January):

$$\bar{T}(h, t) = \frac{T_s(h) + T_w(h)}{2} \left( 1 - \frac{T_s(h) - T_w(h)}{T_s(h) + T_w(h)} \cos(2\pi t / 365) \right), \quad t[\text{days}]; \quad (2)$$

2. Adiabatic BC (2nd kind)  $q_n = 0$  on vertical planes  $Z = 6.0$ ,  $X = \pm 50.0$ ;

3. Convective BC (3rd kind), i.e.:  $q_n = \alpha_c(T - T_e)$  at the remaining surfaces, with ambient temperature  $T_e(t) = T_A(1 - \Delta T / (2T_A) \cdot \cos(2\pi t / 365))$ , where  $T_A = 8$  [°C] is the yearly average temperature,  $\Delta T = 18$  [°C] is the amplitude of monthly averaged temperatures and  $\alpha_c = 2000$  [kJ/(m<sup>2</sup> · day · K)] is the convection coefficient (concrete wall – air).

Fig. 3 shows the FE model (rough mesh is shown) with BC used in the 3D analysis of heat problem and the resulting temperature distribution in [°C] in winter [W] and in summer [S].

In Fig. 4 the histograms of the temperature in points laying on the surface and in the midst of the buttress are shown. A temperature difference of up to  $\Delta T_1 = 7^\circ\text{C}$  appears between the interior and the side surface of the pillar due to the high thermal inertia of the system, related to large dimension of the structure ( $L_{\min} = 5.0$  m). Moreover, the gradients of these strains in the transversal directions are not constant. This explains the main source of thermal stresses and, in consequence, cracking on the lateral surfaces. As a result of subsequent mechanical analysis, the principal stress distributions are shown in Fig. 5 (compression-blue, tension-red). Due to the symmetry, only half of the pillar is considered.

Note, however, that the above low-frequency thermo-mechanical analysis does not indicate any reason for cracking in the head surfaces of the buttress. In this zone, both in summer and in winter, only compressive stresses appear, reaching the value  $\sigma_n \cong 1$  MPa, in the direction tangent to the slopes of the pillar.

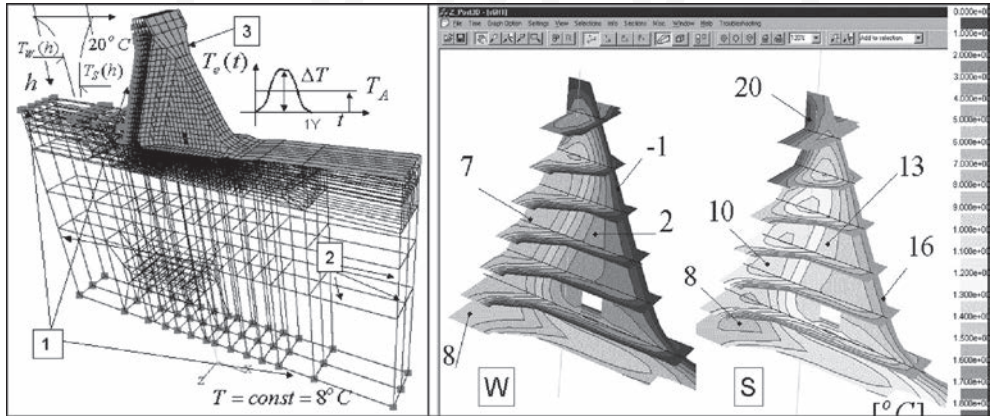


Fig. 3. a) Heat transfer BC. b) Temperature distribution in winter [W] and summer [S]

The temperature field shown in Fig. 3b and Fig. 4 was obtained during the first computational analysis of the dam, conducted by the first author of this paper in 2002 and reported in [5, 6]. In the present analysis, the FE mesh was densified, see Fig. 5, giving however practically the same output.

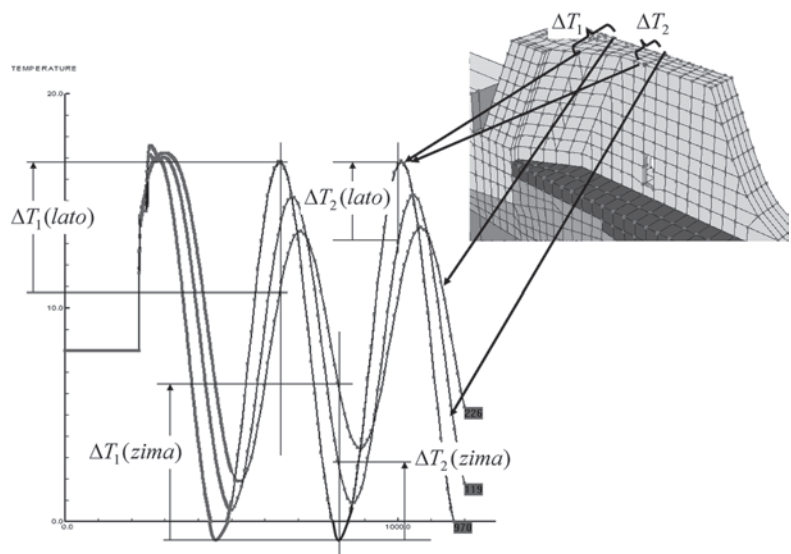


Fig. 4. Histograms of the temperature at selected points

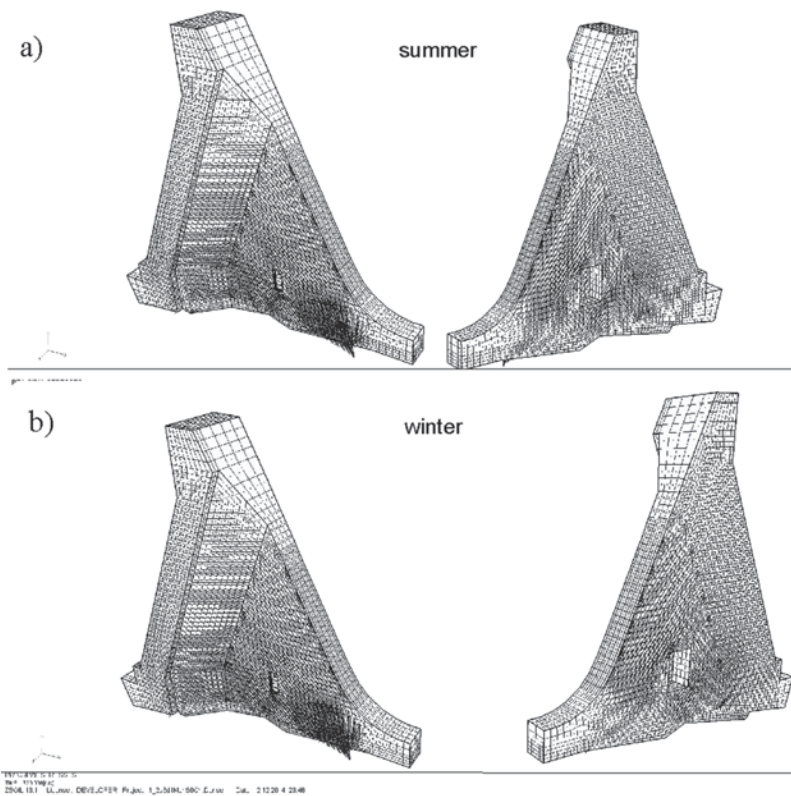


Fig. 5 Principal stresses a) in a summer b) in a winter



## 2.2. Thermal analysis of diurnal (high-frequency) environmental temperature variation and its mechanical impact

In attempting to explain the origin of the multiple cracking of the concrete appearing on the head surface of the buttress, which cannot be result of the yearly temperature cycle, an analysis of daily (high-frequency) environmental temperature variation was undertaken. This is set in the 3D/2D domain which is representative of the whole region close to the head surface. This is shown in Fig. 6. An analysis of high-frequency temperature changes for full model of the section requires also a much denser FE discretisation (estimated size of element in near-surface zone ~10 cm) and time stepping  $dt = 0.1$  day (10 steps per day). These would result in an unacceptably long computation time (few days). Therefore an approximate procedure has been chosen.

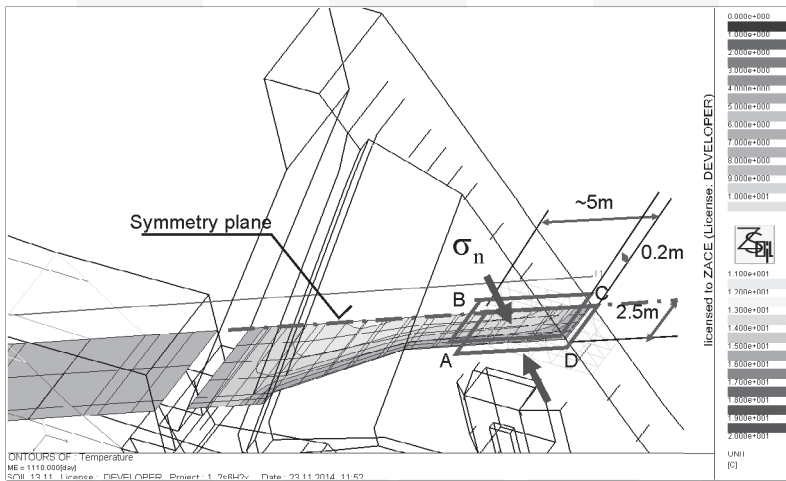


Fig. 6. Localization of the domain for high-frequency thermal and mechanical analysis

Boundary conditions for thermal analysis for the fragment of the dam were adopted as follows:

- along the segment AB – 1-st type of BC, by adopting nodal temperatures as a function of time obtained from the low-frequency solution;
- along the segment BC, on the symmetry plane, 2-nd type of BC (adiabatic,  $q_T = 0$ );
- along the segments CD and AD, 3-rd type of BC (convection). The function of ambient temperature  $T_{eHF}(t)$  describes diurnal variability throughout the year, with yearly averaged temperature  $T_A = 8^\circ\text{C}$  and  $\Delta T = 18^\circ\text{C}$  being the amplitude of daily averages. A term describing the diurnal fluctuation has been added.

$$T_{eHF} = \underbrace{(T_A - \Delta T / 2) \cdot \cos(2\pi t / 365)}_{\text{low-frequency}} + \underbrace{(5 - 2.5 \cdot \cos(2\pi t / 365)) \cdot \sin(2\pi t)}_{\text{high-frequency}}$$

They vary with the seasons, maximum daily amplitude  $\Delta T_{ds} = 15^\circ\text{C}$  (in the summer) and minimum  $\Delta T_{dw} = 5^\circ\text{C}$  (in the winter) were assumed based on meteorological data. The diurnal

cycle was adopted in the form of a sine wave. The ZSoil screen with the function  $T_{eHF}(t)$  is shown in Fig. 7 with high-frequency variability lasting for one year, from the  $t_1 = 555d$  till  $t_2 = 920d$ .

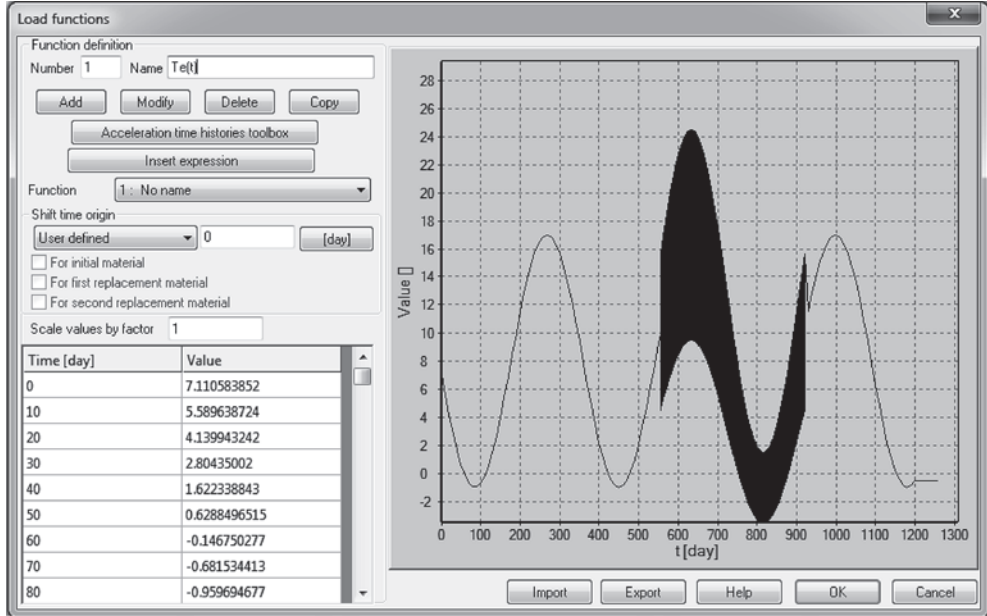


Fig. 7. Ambient temperature function, with high-frequency part  $T_{eHF}(t)$

The following results from thermal and subsequent mechanical analysis for high-frequency temperature variation are shown in Fig. 8: map of the temperature field, principal stress crosses, map of maximum tensile stresses. They are given in 5 selected time instances ( $t + 0.0d$ ,  $t + 0.2d$ ,  $t + 0.4d$ ,  $t + 0.6d$ ,  $t + 0.8d$ ), during one selected day ( $t = 640d$ ) in summer. For that day the maximum of diurnal temperature fluctuation has been reached ( $\Delta T_{ds} = 15^\circ\text{C}$ ).

These results explain the essence of the observed phenomena in the following way: the maximum daily temperature zone shifts from the outer surface into the depths of the massif, temperature gradients reach the value  $\sim 4^\circ\text{C}/0.5\text{ m}$  near the surface. The accompanying thermal strains increments  $\Delta \epsilon_{ii}^o(x, y, z) = \alpha \Delta T(x, y, z)$  have a spatial distribution which do not conform to the compatibility equations (are not-kinematically allowed). As the final deformation must satisfy the compatibility equation, the difference between this and the deformation related to imposed thermal strains is the source of a thermal stress field.

In the present case, these stresses reach values close or equal to the tensile strength of the concrete ( $f_t = 3.00\text{ MPa}$ ). These may be one cause of the cracks at the surface zone. The extent of these cracks is about  $0.5\text{ m}$  in the depth of the massif.



### 3. Final conclusions

The analysis of the thermal and mechanical state in the massive pillar of the dam indicates that there are 2 different mechanisms causing the appearance of cracks in the structure. Both are strongly connected to environmental temperature variation.

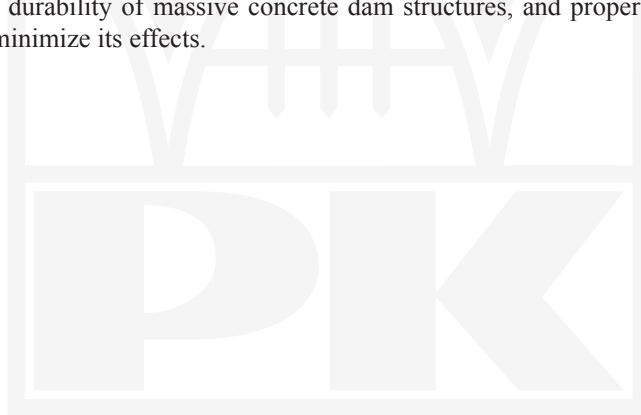
The first mechanism concerns cracking in the central zone of the pillar, which may be explained by temperature differences in the internal points, which remain almost constant during the year, and the temperature and lateral surfaces on the pillar which vary in an annual, low-frequency cycle (winter-summer).

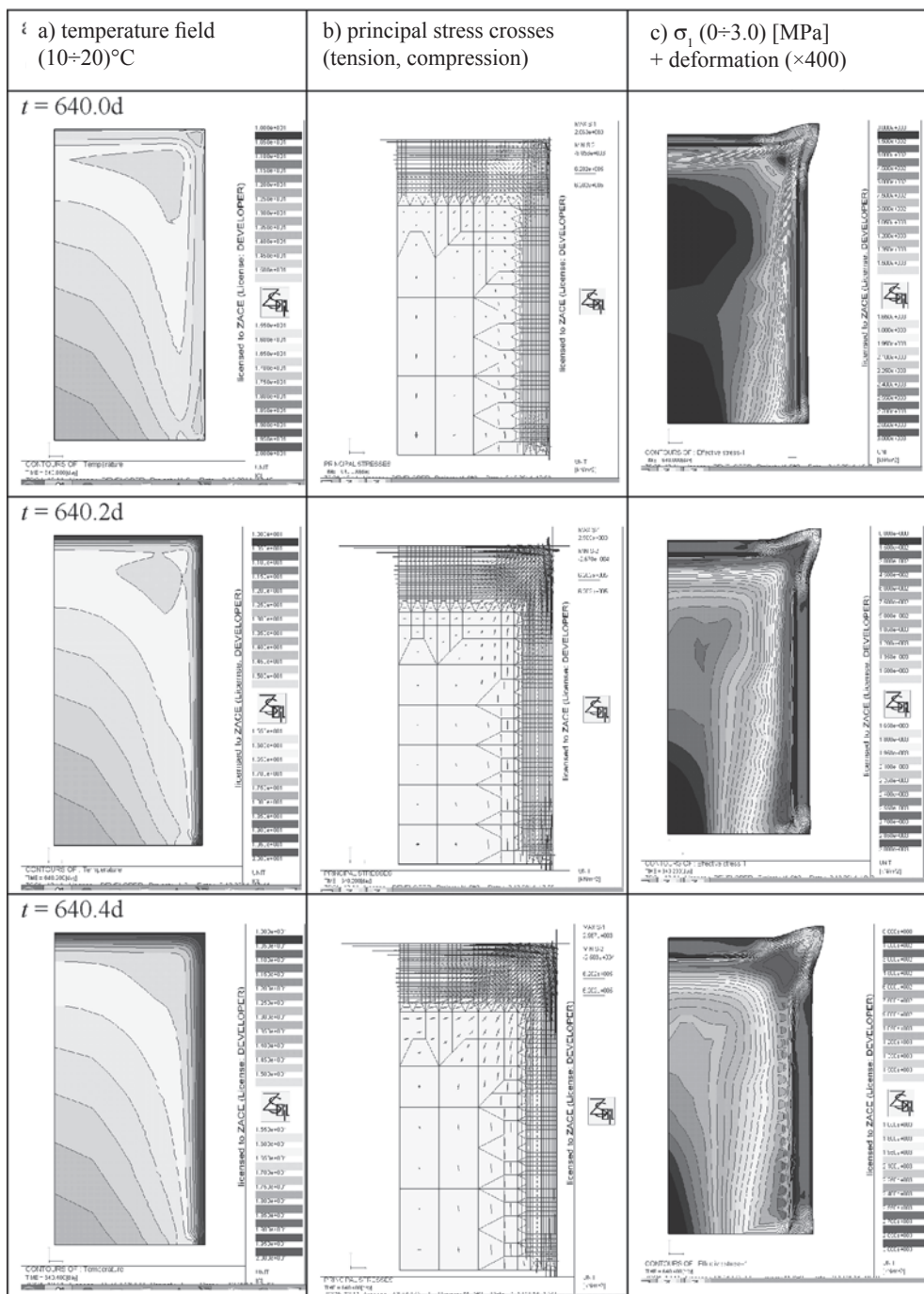
The second, i.e. cracking on the head surfaces, are high-frequency (diurnal) temperature fluctuations (night-day), particularly intensifying in the sunny area, in accordance with the mechanism described in p. 2.2.

These phenomena are stable, they are the consequence of the massiveness of the structure and appear inevitable in a massive concrete structure, but do not threaten its security.

The phenomena of thermal cracking, however, can coexist with other conditions which cause gradual degradation of the structure, such as chemical corrosion of the concrete or frost phenomena. It is noted that penetration of water and its freezing in the already cracked concrete may have a particularly adverse effect on the durability of the structure.

In the long term, the phenomena of thermal cracking may be an important factor influencing the durability of massive concrete dam structures, and proper actions must be undertaken to minimize its effects.





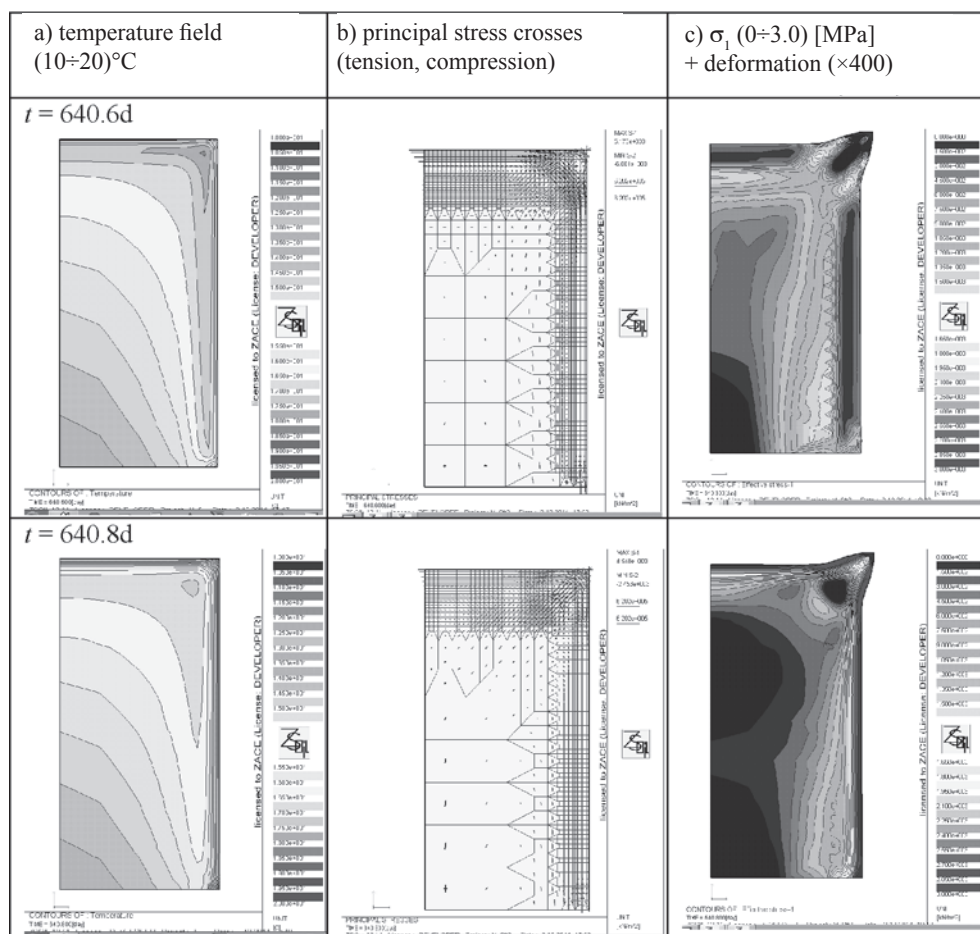


Fig. 8. High-frequency temperature fields and thermal stresses in one daily cycle

## References

- [1] P. Menetrey, *Numerical analysis of punching failure in reinforced concrete structures*, Ph.D. Thesis, EPFL, Lausanne 1994.
- [2] Z. Soil.PC, *Theoretical Manual*, ZACE Services Ltd., Lausanne 2007.
- [3] W. Hrabowski, *Interpretation of the measurement results and evaluation of the safety state of the dam Zatonie* (in Polish), "HRABOWSKI-consulting", 1998.
- [4] A. Urbański, *Numerical modeling of thermal, filtrational and mechanical phenomena in a selected section of a gravity dam*, Proc. of Numerics in Geotechnics & Structures Symposium, Lausanne 2010.

- [5] A. Urbański, W. Hrabowski, J. Hrabowska, *Trójwymiarowe modelowanie numeryczne i analiza in-situ pól termicznych, filtracyjnych i mechanicznych w wybranej sekcji zapory betonowej w Zatoniu*, Materiały Konferencji TKZ Kielce 2003.
- [6] W. Hrabowski, A. Urbański, J. Hrabowska, *Analiza porównawcza pracy najwyższych sekcji zapory w Zatoniu w świetle wyników obserwacji i modelowania komputerowego*, Materiały XIV Konferencji Naukowej – Korbielów' 2002, Wyd. PK 2002.

